Lab Report A-III

Emma Modesitt, Megan Pramojaney, and Nathan McCarley
Department of Physics and Astronomy, The University of North Carolina at Chapel Hill
(Physics 281, Group α)
(Dated: August 15, 2023)

I. THEORETICAL BACKGROUND

A. The Bohr Model of the Hydrogen Atom

The Bohr model of a hydrogen atom is composed of an electron orbiting around a proton [1]. Assuming that radiation reaction effects are negligible, the force exerted on the electron is assumed to be entirely due to the Coulomb force

$$|\vec{F}| = \frac{1}{4\pi\epsilon_0}\frac{q^2}{r^2}, \tag{1}$$

where $\vec{F}$ is the force of the proton on the electron, q is the absolute value of the charge of each subatomic particle, r is the distance between the particles, and ϵ_0 is the permittivity of free space.

Assuming that the electron exhibits uniform circular motion, we know that

$$|\vec{F}| = \frac{mv^2}{r}, \tag{2}$$

where m and v are the mass and velocity of the electron respectively.

Setting Equations 1 and 2 equal to one another, we find v to be

$$v = \sqrt{\frac{1}{4\pi\epsilon_0}\frac{q^2}{rm}}. \tag{3}$$

The kinetic energy of the system T is defined as

$$T = \frac{1}{2}mv^2. \tag{4}$$

The potential energy of the system U is assumed to be entirely electrostatic and is defined as

$$U = -\frac{1}{4\pi\epsilon_0}\frac{q^2}{r}. \tag{5}$$

Substituting our value of v into Equation 4, we can see that the total energy of the system is

$$E = T + U = -\frac{1}{8\pi\epsilon_0}\frac{q^2}{r}. \tag{6}$$

The de Broglie equation defines the electron's wavelength as

$$\lambda_e = \frac{2\pi\hbar}{p}, \tag{7}$$

where p is the momentum of the electron and $\hbar$ is Planck's constant.

The Bohr model takes the electron to be a "circular standing wave" as seen in Figure 1.

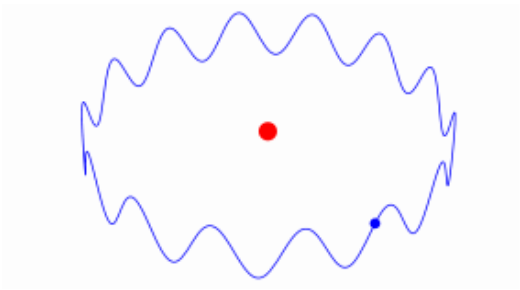

FIG. 1: The electron (blue) as a standing matter wave centered on the proton (red) [1]

Given this assumption, it can be inferred that

$$n\lambda_e = 2\pi r, \tag{8}$$

where n is an positive integer. We can make this inference because the wave closes in on itself after a complete circumference, which must mean that the circumference is an integer multiple of λ_e.

The electron's angular momentum $\vec{L}$ is

$$|\vec{L}| = mvr = pr. \tag{9}$$

By rearranging Equation 7 for p and Equation 8 for λ_e, we can implement these substitutions into Equation 9 to find

$$|\vec{L}| = \frac{2\pi\hbar r}{(\frac{2\pi r}{n})} = n\hbar. \tag{10}$$

Since $|\vec{L}|$ is an integer multiple of $\hbar$, we know that the electron's angular momentum is quantized.

We can then solve for r by equating Equation 9 and 10, then in substituting Equation 3 for v. We find that

$$r = 4\pi\epsilon_0 \frac{\hbar^2 n^2}{mq^2}. \tag{11}$$

Since n can only take on integer values, it follows that r can only take on discrete values. As such, when the electron transitions from a larger radius of energy E_i to a smaller radius of energy E_f, a photon of energy

$$\Delta E = E_i - E_f = 2\pi\hbar f \tag{12}$$

is released, where f is the frequency of the released photon.

Substituting Equation 6 into Equation 12 and rearranging, we obtain

$$f = \frac{mq^4}{64\pi^3\epsilon_0^2\hbar^3}\left(\frac{1}{n_f^2} - \frac{1}{n_i^2}\right). \tag{13}$$

Dividing both sides by c, we obtain

$$\frac{f}{c} = \frac{1}{\lambda} = R\left(\frac{1}{n_f^2} - \frac{1}{n_i^2}\right), \tag{14}$$

where R, Rydberg's constant, is

$$R = \frac{mq^4}{64c\pi^3\epsilon_0^2\hbar^3}. \tag{15}$$

It should be noted that, although heavier atoms than hydrogen also possess discrete emission spectra, their electron-electron interactions are too complex for the Bohr model to accurately depict [1].

B. Gas Discharge Tube Spectroscopy

One way to observe the hydrogen spectrum is through gas discharge tube spectroscopy.

In this process, a strong AC voltage is applied to the electrodes of a hydrogen discharge tube, causing the hydrogen atoms within to ionize. The electrons recombine with protons at random starting energy levels, then proceed to spontaneously decay into lower energy levels. The decay process produces photons with energies equal to the difference between the starting and ending energy levels.

The photons produced can then be spatially separated by frequency using a diffraction grating-based goniometer spectrometer. The diffraction angle θ changes in accordance to the relation

$$j\lambda = d\sin\theta, \tag{16}$$

where j is the integer diffraction order, d is the distance between slits, and λ is the wavelength. Using this relation, we can find λ for each line on the spectrum.

II. RESULTS

We analyzed that data from the goniometer and the hydrogen lamp first. Using Equation 16, we translated the diffraction angle into the wavelength of the emitted photon. The uncertainty in the diffraction angle was $\pm 0.5°$. This uncertainty was then propagated through quadrature to determine the uncertainty of $1/\lambda$. The inverse of the wavelength was plotted as our dependent variable and using the Rydberg equation, $1/n_i^2$ was plotted as the independent variable. This meant that our slope was negative but the magnitude was equal to our experimental Rydberg constant, following Equation 14. The y-intercept of our graph would then be equal to R/n_f^2. Figure 2 shows the linear fit of our data. The uncertainty analysis for the error bars required finding the relative uncertainty of for each diffraction angle and then following the calculations using Equation 16 and Equation 14, the relative uncertainty was translated back into the absolute uncertainty in $1/\lambda$. The uncertainty for our slope and y-intercept were ± 770 mm^{-1} and ± 55 mm^{-1} respectively. These values were determined using the LINEST function in Excel. Since our n_f value was extrapolated from the slope and y-intercept, a propagation of uncertainty in quadrature was used. The y-intercept is represented by b here with

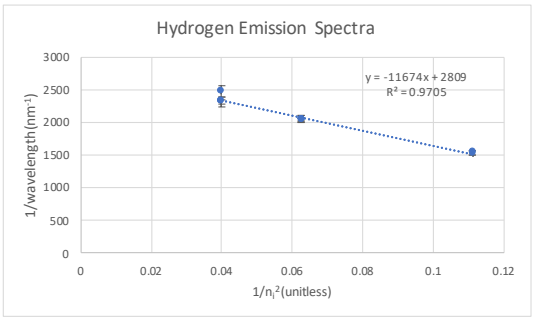

FIG. 2: This graph shows the linear fit of our data with the final energy level held constant at $n_f = 2$ as determined by our y-intercept. The error bars on the data points came from uncertainty in our measurements of the diffraction angle. Using LINEST from Excel, the slope of the graph was -11673.6 mm^{-1}, and the y-intercept was 2809 mm^{-1}.

$$\sigma_{n_f} = \sqrt{\left(\frac{\partial n_f}{\partial R}\right)^2 (\sigma_R)^2 + \left(\frac{\partial n_f}{\partial b}\right)^2 (\sigma_b)^2} \tag{17}$$

being the full quadrature equation. Our final values for our experimental Rydberg constant and n_f were 11674.0 ± 770.0 mm^{-1} and 2.04 ± 0.07 mm^{-1}.

The linear plot in Figure 2 supports the Rydberg formula for hydrogen like atoms, but the analysis of heavier elements spectra is what determines whether this formula is correct for multi-electron atoms. Looking at the helium data first, the Logger-Pro data gave us 6 data points for where peak wavelengths were detected. In Figure 3, we

can see that with two different n_i series, the plot is non-linear when use we the same technique with Equation 14. There are no error bars on this plot because the uncertainty in measurements from the Logger-Pro were not significant.

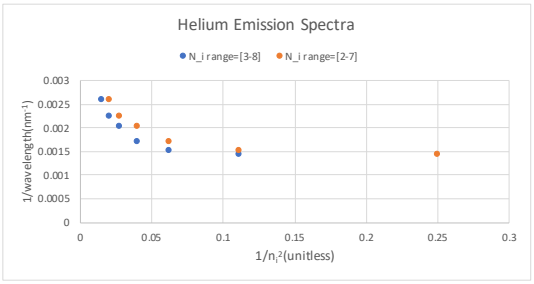

FIG. 3: This graph shows the non-linear fit of our data from the helium vapor lamp with the initial energy levels varying for each of the spectra. The non-linear plot demonstrates that Rydberg's formula does not apply to this heavier heavier element. Since we used a more precise measurement tool for this element, we are also quite sure that no spectra were missed during data collection. This indicates that all photon emissions were recorded and the data should be plotted with increment increases of 1 to n_i.

As with helium, other discharge tubes had spectra recorded with the Logger-Pro. The plots of water vapor and oxygen are displayed in Figure 4 and the plots of nitrogen and mercury are illustrated in Figure 5.

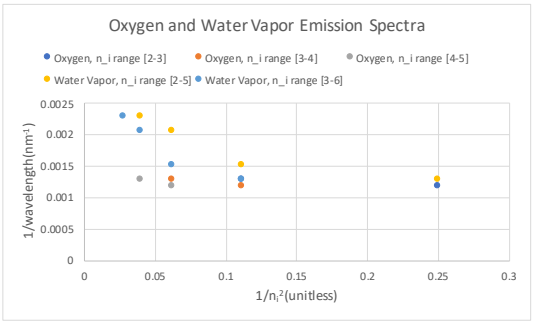

FIG. 4: This graph shows the non-linear fit of our oxygen and Water vapor data with the initial energy levels varying for each of the spectra. The non-linear plot demonstrates that Rydberg's formula does not apply to these heavier elements.

For both oxygen and the water vapor lamps, the Logger-Pro did not pick up many peak wavelengths which is why there are so few data points. The implications of this are described in III.

There were many peak wavelengths picked up by the Logger-Pro digital spectrometer for both the nitrogen and mercury lamps, resulting in a wider data range for these plots than for Figure 4.

III. DISCUSSION AND CONCLUSIONS

The accepted Rydberg constant is $10973731.568160 \pm 0.000021$ m^{-1} [2]. The Rydberg value we calculated of

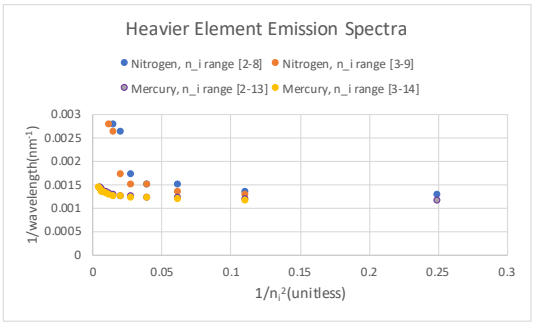

FIG. 5: This graph shows the non-linear fit of our data from nitrogen and mercury peak wavelengths. There are two different series for each element with varying, consecutive initial energy levels. The non-linear plot demonstrates that Rydberg's formula does not apply to nitrogen or mercury, and implies that it will not work for other non-hydrogen-like elements.

11674000 ± 770 m^{-1} is within the bounds of error for the expected value. A possible source of error was in the precision of the angle measurements; although the goniometer allowed us to measure the angles within 0.1 degrees, the viewing piece did not have any marks on it that would have allowed us to perfectly line up the spectral line within the viewer. Our measured angles could have varied between higher or lower than the true angle, which would have respectively decreased or increased our calculated value of R.

The expected value of n_f was 2, which is within the bounds of error for our calculated value of 2.04 ± 0.07. This value could also have been affected by the lack of a completely consistent measurement location in the eyepiece. An angle measurement that was greater than the true angle would result in n_f decreasing.

Examination of other elements revealed non-uniformity in the Rydberg constant, and potential sources of error. The Rydberg constant is known to vary as the elements become heavier — or less like Hydrogen or Helium — because the Bohr model breaks down with the increased number of electrons. Our data in Figure 5 reflects this. Additionally, data from Figure 4 was likely influenced by water vapor's weak emission spectrum. This made it hard to differentiate between peaks, leading to possible error within the measurements.

IV. ACKNOWLEDGMENTS

The experiment was performed by E.M. and N.M., and M.P. recorded the data. E.M. wrote the Results section. M.P. wrote the Theoretical Background section. N.M. wrote the Discussion and Conclusions section. Clarifying questions were answered by Ben Levy.

[1] Lab A-III Manual
https://sakai.unc.edu/access/content/group/41081125-b301-4ad9-8173-970601749ad6/Lab\%20Manuals/Lab\%20A-III\%3A\%20Bohr\%20Model/Lab\%20A-III\%20Bohr\%20Model.pdf
[2] NIST Reference on Constants, Units, and Uncertainty
https://physics.nist.gov/cgi-bin/cuu/Value?ryd